Cellular Physiology and Biochemistry

Cell Physiol Biochem 2012;30:1319-1332
DOI: 10.1159/000343321
Published online: October 22, 2012
Accepted: October 01, 2012

1015-8987/12/0305-1319$38.00/0

Original Paper

Expression and Functional Significance of the Ca^{2+}-Activated Cl^- Channel ANO6 in Dendritic Cells

Kalina Szteyn[a] Evi Schmid[a] Meerim K. Nurbaeva[a] Wenting Yang[a]
Patrick Münzer[a] Karl Kunzelmann[b] Florian Lang[a] Ekaterina Shumilina[a]

[a]Department of Physiology, University of Tübingen, Tübingen; [b]Institut für Physiologie, Universität Regensburg, Regensburg

Key Words
Ano6 • ORCC • TMEM16F • Migration • CCR7

Abstract
Background/Aims: Migration of dendritic cells (DCs), antigen presenting cells that link innate and adaptive immunity, is critical for initiation of immune responses. DC migration is controlled by the activity of different ion channels, which mediate Ca^{2+} flux or set the membrane potential. Moreover, cell migration requires local volume changes at the leading and rear end of travelling cells, which might be mediated by the fluxes of osmotically active solutes, including Cl^-. The present study explored the functional expression, regulation and role of Cl^- channels in mouse bone marrow-derived DCs. ***Methods/Results:*** In whole-cell patch clamp experiments we detected outwardly rectifying Cl^- currents which were activated by elevation of cytosolic Ca^{2+}, triggered either by ionomycin in the presence of extracellular Ca^{2+} or mobilization of Ca^{2+} by IP_3. Most importantly, Ca^{2+}-activated Cl^- channels (CaCCs) were activated by CCL21 (75 ng/ml), an agonist of the chemokine receptor CCR7. The currents showed sensitivity to Cl^- channel blockers such as tannic acid (10 μM), digallic acid (100 μM) and more specific CaCC blockers niflumic acid (300 μM) and AO1 (20 μM). According to RT-PCR and Western blot data, Anoctamin 6 (ANO6) is expressed in DCs. Knock-down of ANO6 with siRNA led to inhibition of CaCC currents in DCs. Moreover, chemokine-induced migration of both immature and LPS-matured DCs was reduced upon ANO6 knock-down. ***Conclusion:*** Our data identify ANO6 as a Ca^{2+}-activated Cl^- channel in mouse DCs, show its activation upon chemokine receptor ligation and establish an important role of ANO6 in chemokine-induced DC migration.

Prof. Dr. Florian Lang
Physiologisches Institut der Universität Tübingen,
Gmelinstr. 5, 72076 Tübingen (Germany)
Tel. +49 7071 29 72194, Fax +49 7071 29 5618, E-Mail florian.lang@uni-tuebingen.de

Introduction

Dendritic cells (DCs) are a heterogenic cell population of hematopoetic origin [1]. Homing of DCs to the tissues is controlled by different chemokines, such as CXCL12 (stromal cell-derived factor 1), a ligand of the receptor CXCR4, expressed by resident cells of normal tissues including mesenchymal, epithelial and endothelial cells [2]. Immature DCs are highly phagocytic and are constantly scanning peripheral tissues for pathogen products and other 'danger' signals, the recognition of which stimulates DC genetic reprogramming and maturation [3]. Upon maturation, DCs acquire a migratory phenotype associated with the upregulation of the chemokine receptor CCR7 and travel through the afferent lymphatics to the lymph nodes attracted by the ligands of CCR7 (chemokines CCL19 and CCL21) [4]. Chemotaxis requires polar differentiation of the cells into a lamellipodium and a cell rear, a process depending on the activity of ion channels and transporters which generate intracellular gradients of Ca^{2+} and H^+ and fluxes of osmotically active Na^+, K^+ and Cl^- [5].

DC migration has been shown to require activity of several ion channels in the plasma membrane including store-operated Ca^{2+} channels [6, 7] and Ca^{2+} permeable TRPV1 [8] channels, voltage-gated K^+ channels [6, 7], Ca^{2+}-activated non-selective cation TRPM4 [9] and KCa3.1 [10] channels.

At least in theory, Cl^- channels, which are, in part, activated by increase of cytosolic Ca^{2+} concentrations, might contribute to the regulation of DC migration. Ca^{2+}-activated Cl^- channels (CaCCs) have been described for the first time in *Xenopus laevis* oocytes [11, 12]. In *Xenopus laevis*, sperm-egg fusion causes release of Ca^{2+} from the stores with subsequent activation of CaCCs, which produce a transient depolarization of the oocyte cell membrane, the so-called "fertilization potential", to prevent polyspermy [13, 14]. In other cell types CaCCs have been shown to be responsible for a plethora of physiological functions. In olfactory [15], taste [16] and photo-receptors [17] they play a role in signal transduction. Additionally, CaCCs are implicated in neuronal [18-20] and cardiac [21-23] excitability as well as regulation of the myogenic tone [24-26] and agonist-stimulated contraction [27] of smooth muscle. Furthermore, CaCC activity in airways and intestinal epithelium participate in stimulation of secretion [28-30].

CaCCs are activated by cytosolic Ca^{2+} with half maximal concentration ranging from 165 nM in Ehrlich ascites tumor cells [31] to 900 nM in *Xenopus* oocytes [26]. At lower Ca^{2+} concentrations CaCC currents show slow activation at positive potentials and fast inactivation at negative potentials [26, 32]. This behaviour results in current-voltage (I-V) relationship that is strongly outwardly rectifying. As the $[Ca^{2+}]_i$ increases, the currents lose their time dependent component and the I-V relationship becomes linear [33, 34]. Depending on the membrane potential and Cl^- concentration gradient, opening of CaCCs can lead to Cl^- efflux or Cl^- influx and cause depolarization or hyperpolarization, respectively [22].

The molecular identity of these channels is not precisely known and over the years several candidate proteins have been proposed. The CLCA family was the first CaCC candidate that has been cloned but even though CLCA channels have been shown to behave as CaCCs when incorporated into an artificial lipid bilayer [35], there are some differences in Ca^{2+}-and voltage-sensitivity, pharmacology and expression profile between CLCA channels and CaCCs [22]. Among other candidates were ClC-3, Tweety and Bestrophins [22]. ClC-3 is regulated by CaMKII [36], but ClC-3-deficient mice show only lack of CaMKII-dependent currents but not of Ca^{2+}-dependent Cl^- conductance [37]. Tweety has been shown to be a Ca^{2+}-regulated maxi Cl^- channel [38], and therefore it might only correspond to the maxi-Cl^- channels present in neurons [39] and skeletal muscle [40]. However, Tweety is not expressed in salivary glands and can not account for the small conductance CaCCs that are typical for acinar cells of secretory glands [38]. Although Bestrophine 1 overexpressed in HEK293 cells generated Ca^{2+} sensitive Cl^- currents [41], CaCC currents are still present in various tissues of bestrophine 1 knockout mice [42-44]. It has been suggested that bestrophins could function as multitask proteins. Besides forming Cl^- channels they could modulate endogenous CaCC activity and regulate other ion channels, for example, voltage-gated Ca^{2+} channels [45, 46].

The only proteins that are clearly CaCCs are members of the Anoctamin (or TMEM16) family [47-49]. The Anoctamin protein family consists of ten members that are expressed in a wide variety of mammalian epithelial tissues. ANO1 is essential for proper development, as ANO1-deficient mice present a severe phenotype and die shortly after birth because of underdeveloped airways [50]. The function of ANO1 and ANO2 as CaCCs is well documented [48, 51-54]. Increasing evidence shows that other members of the ANO family, such as ANO6 and ANO7, are similarly able to generate CaCC currents [50, 55, 56], though in a study on HEK293 cells heterologously expressing ANO proteins, an intracellular localization of ANOs 3-7 has been reported [57]. However, by mutating amino acids in the putative pore-forming domain of ANO6 and expressing ANO6 mutants in HEK293 cells we could show that ANO6 is a membrane channel conducting anions [57]. Moreover, we could demonstrate that ANO6 is a critical component of outwardly rectifying chloride channels (ORCC) in A549 and 9HTE airway epithelial cells and Jurkat T Lymphocytes. In those cells ANO6 is activated by membrane depolarization, proapoptotic stimuli, such as staurosporine or Fas ligand, and activation of ORCC/ANO6 is augmented in the presence of cystic fibrosis transmembrane conductance regulator (CFTR) [55].

In the present study we show for the first time functional expression of CaCCs in murine DCs. We analyze electrophysiological properties of CaCCs in DCs and demonstrate a physiological mechanism of their activation upon ligation of the chemokine receptor CCR7. We demonstrate that ANO6 accounts for detected CaCC conductances in DCs. Finally we show that ANO6 is required for the chemokine-induced migration of both immature and mature DCs.

Materials and Methods

Cell culture

Dendritic cells (DCs) were isolated from bone marrow of 7-12 weeks old mice of C57BL/6 or 129/Sv background as described [7]. Briefly, bone marrow derived cells were flushed out of the cavities from the femur and tibia with PBS. Cells were then washed twice with RPMI and seeded out at a density of 2 x 10^6 cells per 60-mm dish. Cells were cultured for 6 days in RPMI 1640 (GIBCO, Carlsbad) containing: 10 % FCS, 1 % penicillin/streptomycin, 1 % glutamine, 1 % non-essential amino acids (NEAA) and 0.05 % β-mercaptoethanol. Cultures were supplemented with GM-CSF (35 ng/mL, Preprotech Tebu, Germany) and fed with fresh medium containing GM-CSF on days 3 and 6. Experiments were performed on DCs at days 7-11.

Patch clamp

Patch clamp experiments were performed at room temperature in voltage-clamp, fast-whole-cell mode according to Hamill et al. [58]. The cells were continuously superfused through a flow system inserted into the dish. The bath was grounded via a bridge filled with NaCl Ringer solution. Borosilicate glass pipettes (1-3 MOhm tip resistance; GC 150 TF-10, Clark Medical Instruments, Pangbourne, UK) manufactured by a microprocessor-driven DMZ puller (Zeitz, Augsburg, Germany) were used in combination with a MS314 electrical micromanipulator (MW, Märzhäuser, Wetzlar, Germany). The currents were recorded by an EPC-9 amplifier (Heka, Lambrecht, Germany) using Pulse software (Heka) and an ITC-16 Interface (Instrutech, Port Washington, N.Y., USA). Currents were elicited by 200 ms square wave voltage pulses from -50 to +50 mV in 10 mV steps delivered from a holding potential of -30 mV. The currents were recorded with an acquisition frequency of 10 kHz and 3 kHz low-pass filtered. The liquid junction potential ΔE between the pipette and the bath solutions and between the salt bridge and the bath solutions were estimated as described earlier [59]. Data were corrected for the estimated ΔE values.

DCs were superfused with a 'NaCl bath solution' containing: 145 mM/l NaCl, 5 mM/l KCl, 2 mM/l $CaCl_2$, 2 mM/l $MgCl_2$, 20 mM/l glucose, 10 mM/l HEPES/NaOH, pH 7.4. To study the Ca^{2+} sensitivity of the measured current a 'NaCl, 0 Ca^{2+} bath solution' was used, which contained 10 mM/l EGTA and 0 $CaCl_2$. In other experiments extracellular Na^+ was substituted by $NMDG^+$ and the 'NMDG-Cl' bath solution contained: 145 mM/l NMDG-Cl, 2 mM/l $MgCl_2$, 2 mM/l $CaCl_2$, 20 mM/l glucose, 10 mM/l HEPES/NMDG, pH 7.4. To determine the Cl^- permeability of the outward current all chloride salts were isoosmotically replaced by

respective gluconate salts ('Na-gluconate bath solution' or 'NMDG-gluconate bath solution'). In order to induce the Ca^{2+}-activated Cl^- currents, ionomycin (1 μM, Calbiochem, Germany) was applied in 'NMDG-Cl' bath. To prove the Ca^{2+} sensitivity of ionomycin-induced currents 'NMDG-Cl, 0 Ca^{2+} bath solution' was used, which contained 10 mM/l EGTA and 0 $CaCl_2$.

The patch clamp pipettes were filled with either 'CsCl pipette solution' containing: 120 mM/l CsCl, 35 mM/l NaCl, 1 mM/l MgATP, 10 mM/l EGTA, 40 μM/l D-*myo*-inositol-1,4,5-triphosphate (Enzo, Life Sciences), 10 mM/l HEPES/CsOH, pH 7.4; or 'NMDG-Cl pipette solution' containing: 180 mM/l NMDG-Cl, 1 mM/l Mg-ATP, 1 mM/l EGTA, 10 mM/l HEPES, pH 7.2.

Where indicated tannic acid (10 μM, Sigma), AO1 (20 μM, Sygnature Chemical Services Ltd, Nottingham, UK), niflumic acid (300 μM, Sigma) or digallic acid (100 μM, Santa Cruz) were added to the bath solution.

RT-PCR

Total RNA was extracted from mouse DCs in Trizol (Peqlab, Erlangen, Germany) according to the manufacturer's instructions. After DNAse digestion reverse transcription of total RNA was performed using random hexamers (Roche Diagnostics, Penzberg, Germany) and SuperScriptII reverse transcriptase (Invitrogen, Carlsbad, CA, USA). Polymerase chain reaction (PCR) amplification of the respective genes were set up in a total volume of 20 μl using 40 ng of cDNA, 500 nM forward and reverse primer and 2x iTaq Fast SYBR Green (Bio-Rad, Hercules, CA, USA) according to the manufacturer's protocol. Cycling conditions were as follows: initial denaturation at 95°C for 2 min, followed by 40 cycles of 95°C for 15 sec, 55°C for 15 sec and 68°C for 20 sec. For the amplification the following primers were used (5`->3`orientation):

Ano1, fw AGGAATATGAGGGCAACCTG; rev CGACACCATGGATTTTGGTA;
Ano 2, fw ATCCAGCCACCGTCTTCTT; rev ATCCAGCCACCGTCTTCTT;
Ano 3, fw TGATAAAAGAAACACATTTGAAAAGAA; rev AAACATGATATCGGGGCTTG
Ano 4, fw TGGCTTCATTTTTGCTGTTCT; rev CCTGCTTATTTGTTTATCGATCC
Ano 5, fw CAGGGACCACAGTGACCTTT; rev CAGGCGGTATATGAGGATGG
Ano 6, fw GTATGAGGCCCAGTGCAATC; rev TTCCCACAGGTGGTAAATGG
Ano 7, fw TTGGAATCCGAAATGAGGAG; rev GAGCTCCTGTGCCAGCTC
Ano 8, fw CTTGGAGGACCAGCCAATC; rev TGAACTGGAAACACCTGCTG
Ano 9L, fw CAGAGCCCCACATTGACC; rev CTGGGAACTCTCATCATCCTG
Ano 9L/S, fw GTTCCTCGCAAGGCTAAGG; rev CCAGCACTCCAATGGTCTCT
Ano 10, fw CTGATTGTGGTGGCCGTAG; rev TGGCAAATGCGAGTATGAAC
TATA binding protein (Tbp): fw CAAGCTGGAGGTGATCATCG, rev TCCACAGTGCTCTTGAATTCG.

Specificity of PCR products was confirmed by analysis of a melting curve. Real-time PCR amplifications were performed on a CFX96 Real-Time System (Bio-Rad), and all experiments were done in duplicates. Amplification of the housekeeping gene Tbp was performed to standardize the amount of sample RNA. Relative quantification of gene expression was achieved with the ΔΔCt method (where Ct is threshold cycle) as described previously [60]. In addition, PCR products were analysed by agarose gel electrophoresis.

Western blotting

Protein lysates were separated by SDS page 10% gel electrophoresis and transfered onto nitrocellulose membrane. Membrane containing the immobilized proteins was incubated for 1 h in room temperature with 10% non fat milk in Tris-buffered saline-0.1% Tween 20 (TBS-T), followed by over night incubation (4°C) with ANO6 primary antibody (1:300 dilution in 5% non fat milk in TBS-T; Davids, Regensburg). We also used ANO6 antibody (1:200 in BSA, Santa Cruz) and observed similar results (data not shown). The following day membrane was washed 3 times in TBS-T and incubated for 1 h in room temperature with anti-rabbit (Cell Signalling) secondary antibody and washed again in TBS-T. For detection membrane was blotted with ECL reagent (Amersham, Freiburg, Germany), exposed to X-ray film (GE Healthcare) and developed.

Silencing of ANO6

Specific siRNA sequences for ANO6 (CCUCCAUCAUCAGCUUUAUAAUUAU, Invitrogen) and negative control (Silencer® GAPDH siRNA, Ambion, USA) were synthesized and annealed by the manufacturer. siRNA transfection was carried out using the GeneSilencer siRNA transfection reagent (Genlantis, San Diego, CA, USA). 2 x 10^6 cells were washed and plated in 6-well plates in 2 ml of serum-free RPMI 1640. The ANO6 siRNA and the negative control (1000 ng/ml) were incubated with GeneSilencer reagent following the

manufacturer's protocol. Transfection mixture was then added to the wells and incubated over night. The efficiency of silencing was assessed with RT-PCR.

Immunofluorescence

$5x10^4$ DCs were pipetted onto poly-L-Lysine (Sigma-Aldrich) coated microscope slides and incubated at 37°C for 24 h. DCs were fixated by incubating the cells for 20 min at room temperature in 4% paraformaldehyde for 10 min. After blocking for 1 hour with 5% BSA/PBS in room temperature, the cells were incubated overnight at 4°C with ANO6 primary antibodies (1:50). DC slides were incubated with the secondary anti-rabbit-FITC antibody (1:1000, BD Pharmingen), simutaneously, nuclei were stained with DRAQ-5 dye (1:2000, Biostatus, Leicestershire, UK) for 1h at room temperature. The slides were mounted with ProLong Gold antifade reagent (Invitrogen). Images were taken on a Zeiss LSM 5 EXCITER Confocal Laser Scanning Microscope (Carl Zeiss MicroImaging GmbH, Germany) with a water immersion Plan-Neofluar 63_/1.3 NA DIC.

Migration assay

For migration assays transwell inserts (BD Falcon 353097) and BD BioCoatTM MatrigelTM Invasion Chambers (BD Biosciences 354480) were used with a pore diameter size of 8 µm. The transwells were placed in a 24-well cell culture plate containing cell culture medium (750 µl) with or without either CXCL12 (50 ng/ml, Peprotech, for immature DCs) or CCL21 (25 ng/ml, Peprotech, for mature DCs) in the lower chamber. The upper chambers were filled with 500 µl cell culture medium containing immature or LPS (1 µg/ml, 24 h)-matured DCs which were either transfected with a negative control or siRNA for ANO6 in a concentration of 50000 cells/ml. The chamber was placed in a 5% CO_2 37°C incubator for 4 h. In the following step, the transwells were placed in 4% PFA for over night incubation in 4°C, to allow the cells to fix on the membrane. Unattached cells were gently removed with cotton swab, the membrane was then mended on a slide and stained with ProLong® Gold antifade reagent with DAPI (Invitrogen). Cells from five representative areas of each membrane were counted. Spontaneous migration was substracted from the chemokine-induced migration.

Statistics

Data are provided as means ± SE, *n* represents the number of independent experiments. All data were tested for significance using Student's unpaired two-tailed *t*-test or ANOVA and only results with $p < 0.05$ were considered statistically significant.

Results

Ca^{2+}-activated Cl^- channel (CaCC) currents in mouse DCs

In whole-cell patch clamp experiments we studied Ca^{2+}-dependent conductances in mouse bone marrow-derived dendritic cells (DCs) in response to an elevation of cytosolic Ca^{2+} ($[Ca^{2+}]_i$). We first permeabilized the cells with the CsCl-based pipette solution containing IP_3 (40 µM) in order to trigger Ca^{2+} release from the intracellular stores and the subsequent entry of extracellular Ca^{2+} through the store-operated Ca^{2+} (SOC) channels in the plasma membrane. With this pipette solution we observed a fast activation (within 1-2 min following membrane disruption) of outwardly rectifying current with a slope outward conductance of 0.37 ± 0.03 nS and the reversal potential (Erev) of about 0 mV (n = 60) under symmetrical Cl^- solutions (Fig. 1A, C). Replacement of Cl^- in the bath by gluconate ('Na-gluconate bath solution') in paired experiments resulted in a strong reduction of the outward current and a shift of Erev to about +40 mV (n = 22, Fig. 1A, C), demonstrating the Cl^- selectivity of the activated current. The activated current was sensitive to a panel of Cl^- channel inhibitors of a broad spectrum, such as tannic acid (10 µM) and digallic acid (100 µM) and specific inhibitors of Ca^{2+}-activated Cl^- channels (CaCCs) [61]: AO1 (20 µM) and niflumic acid (300 µM) (Fig. 1B, D, E). We then removed Ca^{2+} from the bath solution in order to test whether Ca^{2+} released from internal stores was sufficient to induce CaCC currents when no extracellular Ca^{2+} entered the cells. The outwardly rectifying current was induced within 4-5 min following achievement of

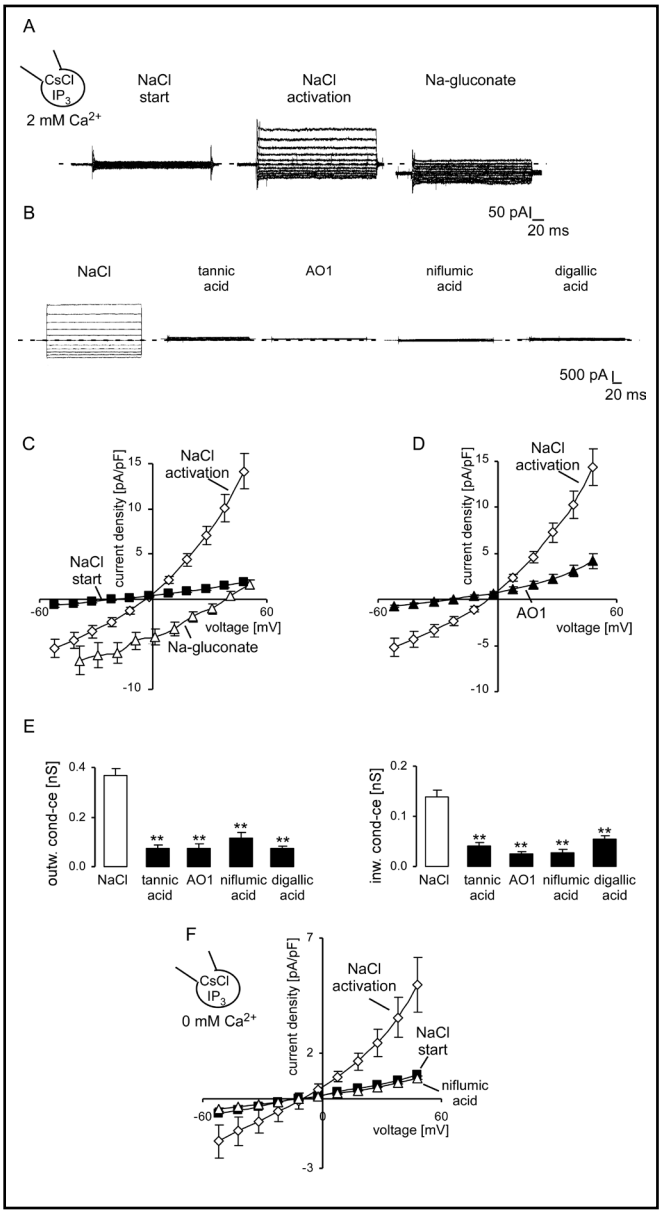

Fig. 1. Cl^- currents are activated by IP_3 in DCs. A. Current tracings from a dendritic cell (DC) recorded with inositol-1,4,5-triphosphate (IP_3, 40 μM)-containing CsCl pipette solution immediately after reaching the whole-cell mode (start, left), in 2 min upon full current activation (middle) in NaCl bath solution containing 2 mM/l $CaCl_2$ and then after substitution of bath NaCl with Na-gluconate (right). Currents were obtained in fast whole-cell voltage-clamp mode. The membrane potential was held at -30 mV and currents were elicited by 200-ms square pulses to test potentials between -50 and +50 mV in 10 mV steps; zero current is indicated by a dashed line. B. Representative current tracings recorded from DCs with IP_3-containing CsCl pipette and NaCl bath solutions upon full current activation (left) and after application of Cl^- channel blockers: tannic acid (10 μM), AO1 (20 μM), niflumic acid (300 μM) and digallic acid (100 μM). Currents were recorded as in A. C. Mean current-voltage (I-V) relations (± SE, n = 22-26) of DCs (recorded as in A) immediately after reaching the whole-cell mode (NaCl start, closed squares), in 1-2 min upon full current activation in NaCl (NaCl activation, open almonds) and in Na-gluconate (open triangles) bath solutions. D. Mean I-V relations (± SE, n = 26) of DCs recorded as in B upon full current activation (open almonds) and after application of the Cl^- channel blocker AO1 (20 μM). E. Mean outward (left) and inward (right) conductances (± SE) calculated from the individual I-V relations (as in D) by linear regression of outward current between +10 and +50 mV and of inward current between -10 and -50 mV, respectively, in DCs upon full current activation (NaCl) and after application of Cl^- channel blockers: tannic acid (10 μM, n = 15), AO1 (20 μM, n = 26), niflumic acid (300 μM, n = 7) and digallic acid (100 μM, n = 12). ** ($p<0.01$), ANOVA, Dunnett test. F. Mean current-voltage (I-V) relations (± SE, n = 6-8) of DCs recorded with IP_3-containing CsCl pipette solution and Ca^{2+}-free NaCl bath solution immediately after reaching the whole-cell mode (NaCl start, closed squares), in 4 min upon full current activation (NaCl activation, open almonds) and then upon inhibition of the current with niflumic acid (300 μM, open triangles).

the whole cell configuration (Fig. 1F), however the slope outward conductance was only 0.10 ± 0.03 nS (n = 8) which was significantly lower (P = 0.0028) than in Ca^{2+}- containing bath. The current was inhibited by niflumic acid (300 μM, Fig. 1F).

To further explore the Ca^{2+} dependence of detected currents, we exposed DCs to the Ca^{2+} ionophore ionomycin in Ca^{2+} containing and Ca^{2+} free extracellular solutions (Fig. 2).

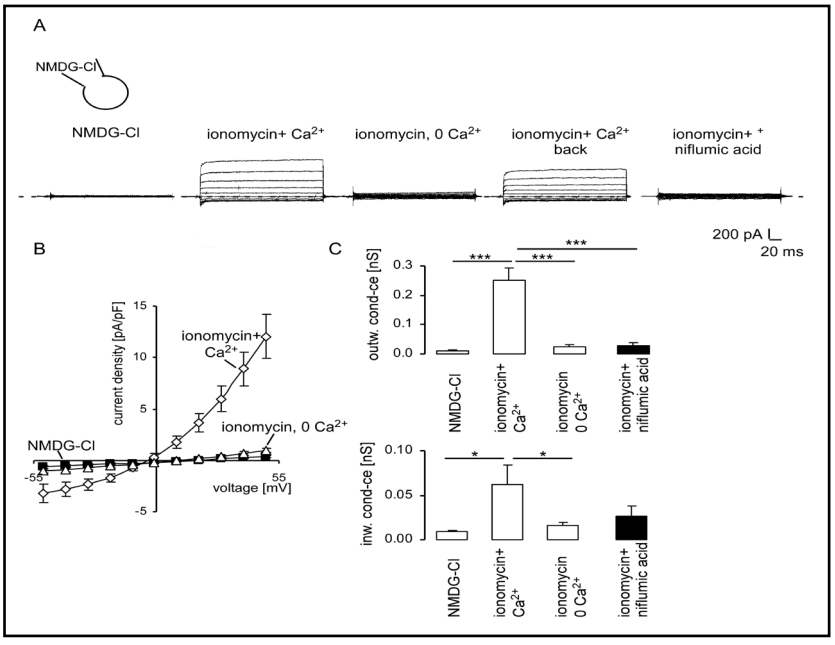

Fig. 2. Cl^- currents are activated by ionomycin-induced Ca^{2+} increase in DCs. A. Current tracings from a DC recorded with NMDG-Cl pipette solution before (1st trace) and after application of ionomycin (1 µM) in Ca^{2+}-containing (2 mM $CaCl_2$, 2nd and 4th traces), in Ca^{2+}-free (10 mM EGTA, 3rd trace) and in Ca^{2+}- and niflumic acid (300 µM)-containing (last trace) NMDG-Cl bath solution. B. Mean I-V relations (± SE, n = 11-18) of DCs recorded as in A before (NMDG-Cl, closed squares) and after application of ionomycin (1 µM) in Ca^{2+}-containing (ionomycin + Ca^{2+}, open almonds) and then in Ca^{2+}-free (ionomycin, 0 Ca^{2+}, open triangles) NMDG-Cl bath solution. C. Mean outward (upper panel) and inward (lower pannel) conductances (± SE, n = 11-18) calculated from the individual I-V relations (as in B) by linear regression of outward current between +10 and +50 mV and of inward current between -10 and -50 mV, respectively, in DCs before (NMDG-Cl) and after application of ionomycin (1 µM) in Ca^{2+}-containing (ionomycin + Ca^{2+}), in Ca^{2+}-free (ionomycin, 0 Ca^{2+}) and in Ca^{2+}- and niflumic acid (300 µM)-containing (ionomycin+niflumic acid) NMDG-Cl bath solution. * ($p<0.05$) and *** ($p<0.001$), ANOVA, Bonferroni test.

These and following patch-clamp experiments were performed using pipette and bath solutions containing NMDG as a Na^+ and K^+ replacement, and Cl^- as the major permeable ion ('NMDG-Cl pipette and bath solutions'). In the presence of extracellular Ca^{2+}, ionomycin (1 µM) induced fast outwardly rectifying current activation (Fig. 2). After full current activation was reached, the Ca^{2+} containing extracellular solution was replaced in paired experiments with a nominally Ca^{2+} free solution (0 Ca^{2+}, 10 mM EGTA, Fig. 2). The Ca^{2+} removal was followed by a significant decline, in both, outward and inward currents (Fig. 2), indicating that elevated intracellular Ca^{2+} via the Ca^{2+} ionophore was responsible for the Cl^- current activation. Readdition of Ca^{2+} into the bath solution led to reactivation of the current which was subsequently inhibited with niflumic acid (300 µM, Fig. 2A, C). Therefore, mouse DCs express functional CaCCs.

To explore whether CaCCs are activated by physiological stimuli, additional experiments were performed with the chemokine CCL21, a ligand of CCR7 chemokine receptor expressed on DC cell membrane and triggering chemotactic responses and guiding mature DCs to the T zones of secondary lymphoid organs [62]. It has been shown that CCR7 stimulation leads to an increase of $[Ca^{2+}]_i$ in DCs [9]. According to patch clamp experiments, CCL21 applied to the bath solution in the concentration of 75 ng/ml, which is known to activate Ca^{2+} entry in DCs [9] activated CaCCs in 75% of measured cells. The currents were rapidly activated by CCL21, showed a very strong outward rectification and a fast rundown (Fig. 3). Upon stabilization of currents after primary activation, Cl^- in the bath was substituted by gluconate, which resulted in a strong decrease of the outward currents and a shift of Erev towards positive potentials, indicating Cl^- selectivity of CCL21-activated current (Fig. 3). The outward currents were restored on return to Cl^- bath solution to the levels at which they stabilized after primary activation (Fig. 3A).

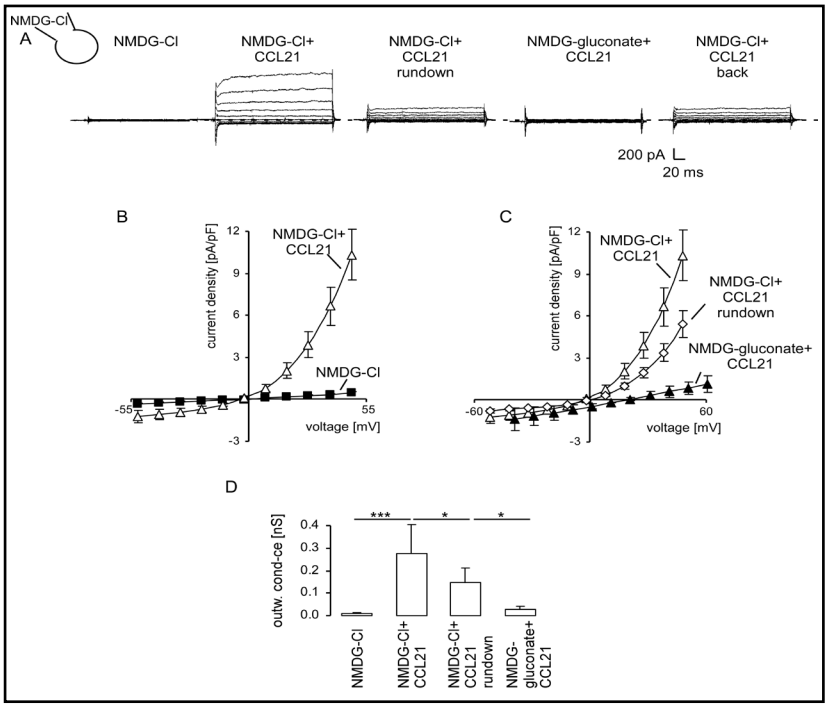

Fig. 3. Cl^- currents are activated by CCL21 in DCs. A. Current tracings from a DC recorded with NMDG-Cl pipette solution before (1st trace) and after application of CCL21 (75 ng/ml, 2nd,3rd and 5th traces) 30 s (2nd trace) and 4 min (3rd trace, showing current rundown) after CCL21 application in NMDG-Cl bath solution, after substitution of bath NMDG-Cl with NMDG-gluconate (4th trace) and after a wash-out of Na-gluconate with NMDG-Cl (5th trace). B. Mean I-V relations (± SE, n = 9) of DCs (recorded as in A) before (NMDG-Cl, closed squares) and 30 s after (NMDG-Cl+CCL21, open triangles) application of CCL21 (75 ng/ml) in NMDG-Cl bath solution. C. Mean I-V relations (± SE, n = 2-9) of DCs (recorded as in A) 30 s (NMDG-Cl+CCL21, open triangles) and 4 min (NMDG-Cl+CCL21 rundown,open almonds) after application of CCL21 (75 ng/ml) in NMDG-Cl bath solution and after substitution of bath NMDG-Cl with NMDG-gluconate (NMDG-gluconate+CCL21, closed triangles). D. Mean outward conductances (± SE, n = 2-9) calculated from the individual I-V relations (as in B and C) by linear regression of the current between +10 and +50 mV in DCs before (NMDG-Cl) and after application of CCL21 (75 ng/ml) 30 s (NMDG-Cl+CCL21) and 4 min (NMDG-Cl+CCL21 rundown) after CCL21 application in NMDG-Cl bath solution and after substitution of bath NMDG-Cl with NMDG-gluconate (NMDG-gluconate+CCL21). * ($p<0.05$) and *** ($p<0.001$), ANOVA, Bonferroni test.

Expression of Anoctamins in DCs

Some of the members of the Anoctamin (ANO) protein family have been identified as Ca^{2+}-activated Cl^- channels [47-49, 53, 54]. The ANO protein family consists of ten members with tissue specific patterns of expression [50]. To explore whether ANO channels are expressed in DCs and could contribute to or account for the detected CaCC conductances, we performed RT-PCR analysis with primers specific for all ten members of the ANO family. RT-PCR revealed mRNA expression of ANO6, ANO8 and ANO10 in mouse DCs with ANO6 having the highest expression level (Fig. 4A, B). Among these ANO members only ANO6 has been shown to generate a Ca^{2+}-activated Cl^- channel [50]. Accordingly, western blotting was performed with ANO6 antibodies and demonstrated that ANO6 protein was indeed expressed in mouse DCs (Fig. 4C).

ANO6 dependence of AO1-sensitive outwardly-rectifying currents

Next we performed whole-cell patch clamp experiments in DCs in which ANO6 was silenced with ANO6-siRNA. Knock-down efficiency was about 58% as tested with real-time RT-PCR (Fig. 5B) and confirmed by immunofluorescent staining of the cells (Fig. 5C). Within 1-2 min following membrane disruption in experiments using IP_3-containing pipette solution, about 80% of control cells demonstrated outwardly-rectifying currents sensitive to AO1 (Fig. 5A). In contrast about 70% of DCs (15 out of 22 cells) with silenced ANO6 showed no development of AO1-sensitive outwardly-rectifying currents within 5-10 min of

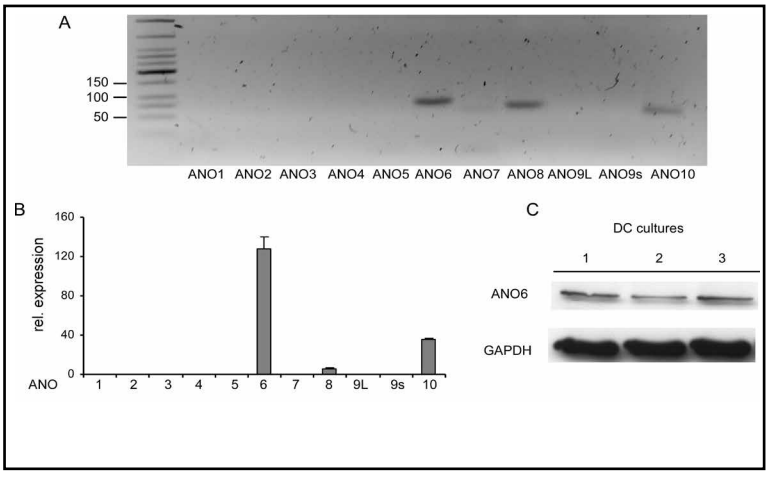

Fig. 4. Expression of Anoctamins in mouse DCs. A. Agarose gel with PCR products specific for Anoctamins 1-10 amplified from cDNA isolated from mouse DCs. B. ANO1-10 mRNA levels (± SE, n = 3) determined after isolation from mouse DCs and assessed by real-time PCR using TBP mRNA as a reference gene. C. Western Blot analysis of ANO6 expression in whole cell protein lysates extracted from mouse DCs.

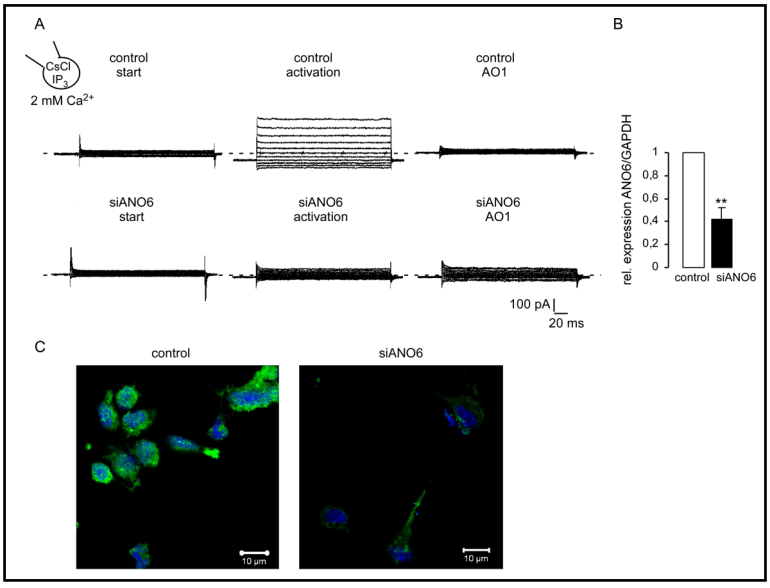

Fig. 5. Knock-down of ANO6 inhibits CaCC currents in DCs. A. Current tracings recorded with IP_3-containing CsCl pipette and NaCl bath solutions immediately after reaching the whole-cell mode (start, left), upon full current activation (activation, middle) and after application of CaCC blocker AO1 (20 µM) in control DCs (upper panel, representative for 80% (17 out of 21) measured cells) and in siANO6-DCs (lower panel, representative for 69% (15 out of 22) measured cells). Zero current is indicated by a dashed line. B. ANO6 mRNA levels (± SE, n = 4) determined in control DCs (empty vector-transfected, open bars) and siANO6-DCs (closed bars) and assessed by real-time PCR using GAPDH mRNA as a reference gene. ** ($p<0.01$), one sample *t*-test. C. Confocal microscopy of ANO6 abundance in DCs transfected with empty vector (control) and siANO6-DCs. The nuclei are stained with DRAQ5 (blue) and ANO6 with FITC-conjugated secondary antibody (green).

recording (Fig. 5A). In 7 out of 22 measured DCs with silenced ANO6 normal CaCC currents indistinguishable from control DCs were observed.

ANO6 dependent migration of DCs

Since CaCCs are activated upon ligation of the chemokine receptor CCR7, we further analyzed migration of immature and mature DCs upon silencing of ANO6. To induce DC maturation, cells were incubated with LPS (1 µg/ml) for 24h prior to assay performance. Migration was tested in both, the absence and presence of the chemokines CXCL12 (50 ng/ml) in immature DCs and CCL21 (25 ng/ml) in LPS-matured cells. In a transwell migration assay chemokine-induced migration of both immature and mature DCs was strongly impaired by siRNA for ANO6 (Fig. 6).

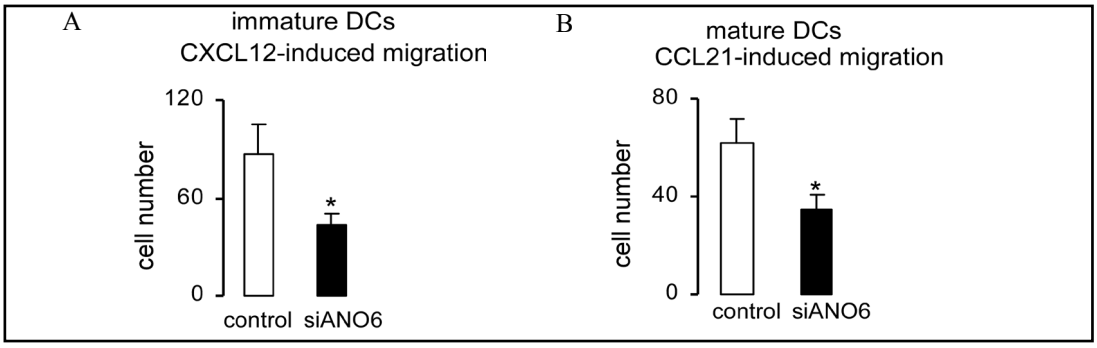

Fig. 6. Chemokine-induced DC migration is inhibited by knock-down of ANO6. Number (± SE, n = 17-26) of immature (A) or mature (B) DCs migrating towards the chemokine CXCL12 (50 ng/ml, A) or CCL21 (25 ng/ml, B), respectively, measured in transwell migration assay with control DCs (empty vector-transfected, open bars) and siANO6-DCs (closed bars). Maturation of DCs was induced by LPS (1 μg/ml, 24 h). The data are corrected for spontaneous migration. * ($p<0.05$), unpaired two-tailed *t*-test.

Discussion

The current study is the first to identify Ca^{2+}-activated Cl^- channel (CaCC) ANO6 in DCs and to examine its role in DC function. In whole-cell patch clamp experiments performed on mouse DCs, we demonstrated outwardly rectifying Cl^- currents activated by elevation of cytosolic Ca^{2+}, triggered either by the ionophore ionomycin in the presence of extracellular Ca^{2+}, or by IP_3-dependent Ca^{2+} mobilization. Moreover, we detected a physiological mechanism of CaCC activation in DCs upon stimulation of the chemokine receptor CCR7. Recorded currents show all the hallmarks of endogenous CaCCs. Like in neurons [63], cardiomyocytes [64] and *Xenopus laevis* oocytes [26, 65] both, Ca^{2+} entry from extracellular environment and Ca^{2+} release from intracellular stores, were able to activate CaCCs in DCs.

When Ca^{2+}-activated Cl^- currents were induced by the chemokine CCL21, the current-voltage (I-V) relationship showed stronger outward rectification, if compared to more linear I-V curves when the trigger was the Ca^{2+} ionophore ionomycin or IP_3 in the pipette solution. This was consistent with previously described features of CaCCs, that the outward rectification is lost with higher $[Ca^{2+}]_i$ [22, 26, 33, 65], as extracellular ionomycin or IP_3 in the pipette would induce much higher and/or more prolonged increase of $[Ca^{2+}]_i$ than CCL21. Even though specificity of CaCC inhibitors is limited, the currents detected in DCs showed sensitivity to most commonly used Cl^- channel blockers, including AO1, a specific inhibitor of the anoctamin CaCC family [61].

The molecular identity of CaCCs stirred up, over the years, a lot of controversy but since identification of ANO1 as Ca^{2+}-activated Cl^- channel by three independent groups in 2008 [47-49], the mystery seems to be, at least partly, solved. We detected expression of three members of the Anoctamin family ANO6, ANO8, ANO10 in mouse DCs. Among those, only ANO6 has previously been shown to generate Ca^{2+}-activated Cl^- currents whereas ANO8 has not produced any detectable current, when expressed in FTR cells. ANO10 has even suppressed baseline Cl^- conductance and its co-expression with ANO1 caused decrease of the ANO1-generated currents [50]. In the present study knock-down of ANO6 with siRNA abrogated CaCC currents in almost 70% of measured cells, which was consistent with the efficiency of knock-down, that was about 58% in our experiments. In the light of those observations we suggest that ANO6 is responsible for Ca^{2+}-activated Cl^- currents detected in DCs.

Even though the molecular identity of representatives of CaCCs has been defined only recently [47-49], their functions in many cells and tissue models have been investigated for almost three decades. In cells of haematopoetic origin, CaCC currents have been characterized in neutrophils [66], macrophages [67], Jurkat lymphocytes [68] and human mast cell line HMC-1 [69]. In these studies CaCCs were activated by Ca^{2+} ionophore or by dialyzing the cell

with high concentrations of Ca^{2+} in the patch pipette. We have recently shown an important function of ANO6 as an essential component of the outwardly rectifying chloride channel (ORCC) in airway epithelial cells and Jurkat T lymphocytes [55]. ANO6/ORCC is activated upon membrane depolarization and apoptosis. In addition the cystic fibrosis transmembrane conductance regulator (CFTR) in presence of cAMP augments ANO6/ORCC currents [55]. Our present study provides another physiological mechanism of ANO6 activation in DCs, through the stimulation of the chemokine receptor CCR7.

In contrast to our present investigation on DCs, ANO6/ORCC in airway epithelial cells and Jurkat T lymphocytes is not Ca^{2+}-dependent [55]. This discrepancy may result from ANO6 forming variable oligomeric complexes and/or associating with variable accessory proteins in different cell types. As we have previously shown, ANO6 is able to generate the Ca^{2+} activated Cl^- currents in ANO6-overexpressing FRT cells [50, 56].

Migration is one of the essential functions of DCs. The process is induced by chemoattractants present at infection/inflammation sites as well as expressed by secondary lymphoid organs [62]. Our results show that the chemokine-induced migration of both immature (towards the chemokine CXCL12) and mature (towards the chemokine CCL21) DCs requires activity of ANO6. A possible mechanism of ANO6-regulated DC migration may include ANO6-mediated local volume changes required for lamellipodium growth and/or cell rear end retraction by uptake and/or efflux of osmotically active Cl^-. As a matter of fact, hypotonic stimulus has been shown to cause the $[Ca^{2+}]_i$ rise in mouse astrocytes in the immediate vicinity of open Ca^{2+}-permeable channels, so called Ca^{2+} nanodomains, which generation is triggered by an autocrine action of ATP [70]. This $[Ca^{2+}]_i$ rise in Ca^{2+} nanodomains induces ORCC channel activation [70]. Moreover in astrocytes, inflammatory chemical mediator, bradykinin [71] and extracellular ATP [70] lead to ORCC activation by $[Ca^{2+}]_i$ rise in Ca^{2+} nanodomains without cell swelling.

ANO6 may further provide a positive feedback to store-operated Ca^{2+} influx, which is required for DC migration [7]. The resting membrane potential of mouse DCs has been estimated as ~ -20 mV [7] that is most probably more positive than the equilibrium Cl^- potential. Thus opening of ANO6 channels would lead to hyperpolarization of the cell membrane, providing electrical driving force for Ca^{2+} entry through the store-operated Ca^{2+} channels, which are steeply inwardly rectifying [72]. CaCCs supporting Ca^{2+} influx have been also demonstrated in pulmonary arterial smooth muscle [73] and Cajal [74] cells.

In summary, we identified novel Ca^{2+}-activated Cl^- channels in bone marrow derived murine DCs. We demonstrated that these channels are activated upon ligation of the chemokine receptor CCR7. By siRNA knock-down approach we could show that ANO6 isoform of the anoctamin protein family accounts for the measured currents. Moreover, ANO6 played an important role in the chemokine-induced migration of both immature and mature DCs.

Acknowledgemens

This study was supported by the contract grant sponsor: Deutsche Forschungsgemeinschaft; Contract grant number: SFB699A7.

References

1 Shortman K, Liu YJ: Mouse and human dendritic cell subtypes. Nat Rev Immunol 2002;2:151-161.
2 Murdoch C: Cxcr4: Chemokine receptor extraordinaire. Immunol Rev 2000;177:175-184.
3 Banchereau J, Briere F, Caux C, Davoust J, Lebecque S, Liu YJ, Pulendran B, Palucka K: Immunobiology of dendritic cells. Annu Rev Immunol 2000;18:767-811.

4 Randolph GJ, Ochando J, Partida-Sanchez S: Migration of dendritic cell subsets and their precursors. Annu Rev Immunol 2008;26:293-316.
5 Shumilina E, Huber SM, Lang F: Ca^{2+} signaling in the regulation of dendritic cell functions. Am J Physiol Cell Physiol 2011;300:C1205-1214.
6 Xuan NT, Shumilina E, Matzner N, Zemtsova IM, Biedermann T, Goetz F, Lang F: Ca^{2+}-dependent functions in peptidoglycan-stimulated mouse dendritic cells. Cell Physiol Biochem 2009;24:167-176.
7 Matzner N, Zemtsova IM, Nguyen TX, Duszenko M, Shumilina E, Lang F: Ion channels modulating mouse dendritic cell functions. J Immunol 2008;181:6803-6809.
8 Basu S, Srivastava P: Immunological role of neuronal receptor vanilloid receptor 1 expressed on dendritic cells. Proc Natl Acad Sci USA 2005;102:5120-5125.
9 Barbet G, Demion M, Moura IC, Serafini N, Leger T, Vrtovsnik F, Monteiro RC, Guinamard R, Kinet JP, Launay P: The calcium-activated nonselective cation channel trpm4 is essential for the migration but not the maturation of dendritic cells. Nat Immunol 2008;9:1148-1156.
10 Shao Z, Makinde TO, Agrawal DK: Calcium-activated potassium channel kca3.1 in lung dendritic cell migration. Am J Respir Cell Mol Biol 2011;45:962-968.
11 Miledi R: A calcium-dependent transient outward current in xenopus laevis oocytes. Proc R Soc Lond B Biol Sci 1982;215:491-497.
12 Barish ME: A transient calcium-dependent chloride current in the immature xenopus oocyte. J Physiol 1983;342:309-325.
13 Webb DJ, Nuccitelli R: A comparative study of the membrane potential from before fertilization through early cleavage in two frogs, rana pipiens and xenopus laevis. Comp Biochem Physiol A Comp Physiol 1985;82:35-42.
14 Fontanilla RA, Nuccitelli R: Characterization of the sperm-induced calcium wave in xenopus eggs using confocal microscopy. Biophys J 1998;75:2079-2087.
15 Kurahashi T, Yau KW: Olfactory transduction. Tale of an unusual chloride current. Curr Biol 1994;4:256-258.
16 Herness MS, Sun XD: Characterization of chloride currents and their noradrenergic modulation in rat taste receptor cells. J Neurophysiol 1999;82:260-271.
17 Barnes S: After transduction: Response shaping and control of transmission by ion channels of the photoreceptor inner segments. Neuroscience 1994;58:447-459.
18 Owen DG, Segal M, Barker JL: A ca-dependent cl- conductance in cultured mouse spinal neurones. Nature 1984;311:567-570.
19 Barker JL, Ransom BR: Amino acid pharmacology of mammalian central neurones grown in tissue culture. J Physiol 1978;280:331-354.
20 Andre S, Boukhaddaoui H, Campo B, Al-Jumaily M, Mayeux V, Greuet D, Valmier J, Scamps F: Axotomy-induced expression of calcium-activated chloride current in subpopulations of mouse dorsal root ganglion neurons. J Neurophysiol 2003;90:3764-3773.
21 Hume JR, Duan D, Collier ML, Yamazaki J, Horowitz B: Anion transport in heart. Physiol Rev 2000;80:31-81.
22 Hartzell C, Putzier I, Arreola J: Calcium-activated chloride channels. Annu Rev Physiol 2005;67:719-758.
23 Verkerk AO, Tan HL, Ravesloot JH: Ca^{2+}-activated cl- current reduces transmural electrical heterogeneity within the rabbit left ventricle. Acta Physiol Scand 2004;180:239-247.
24 Large WA, Wang Q: Characteristics and physiological role of the Ca^{2+}-activated Cl^- conductance in smooth muscle. Am J Physiol 1996;271:C435-454.
25 Angermann JE, Sanguinetti AR, Kenyon JL, Leblanc N, Greenwood IA: Mechanism of the inhibition of Ca^{2+}-activated Cl^- currents by phosphorylation in pulmonary arterial smooth muscle cells. J Gen Physiol 2006;128:73-87.
26 Kuruma A, Hartzell HC: Bimodal control of a Ca^{2+}-activated Cl^- channel by different Ca^{2+}signals. J Gen Physiol 2000;115:59-80.
27 Davis MJ, Hill MA: Signaling mechanisms underlying the vascular myogenic response. Physiol Rev 1999;79:387-423.
28 Barrett KE: Positive and negative regulation of chloride secretion in t84 cells. Am J Physiol 1993;265:C859-868.

29 Gabriel SE, Makhlina M, Martsen E, Thomas EJ, Lethem MI, Boucher RC: Permeabilization via the p2x7 purinoreceptor reveals the presence of a Ca^{2+}-activated Cl^- conductance in the apical membrane of murine tracheal epithelial cells. J Biol Chem 2000;275:35028-35033.
30 Kunzelmann K, Milenkovic VM, Spitzner M, Soria RB, Schreiber R: Calcium-dependent chloride conductance in epithelia: Is there a contribution by bestrophin? Pflugers Arch 2007;454:879-889.
31 Papassotiriou J, Eggermont J, Droogmans G, Nilius B: Ca^{2+}-activated Cl^- channels in ehrlich ascites tumor cells are distinct from mclca1, 2 and 3. Pflugers Arch 2001;442:273-279.
32 Nilius B, Prenen J, Voets T, Van den Bremt K, Eggermont J, Droogmans G: Kinetic and pharmacological properties of the calcium-activated chloride-current in macrovascular endothelial cells. Cell calcium 1997;22:53-63.
33 Chen Y, An H, Li T, Liu Y, Gao C, Guo P, Zhang H, Zhan Y: Direct or indirect regulation of calcium-activated chloride channel by calcium. J Membr Biol 2011;240:121-129.
34 Evans MG, Marty A: Calcium-dependent chloride currents in isolated cells from rat lacrimal glands. J Physiol 1986;378:437-460.
35 Cunningham SA, Awayda MS, Bubien JK, Ismailov II, Arrate MP, Berdiev BK, Benos DJ, Fuller CM: Cloning of an epithelial chloride channel from bovine trachea. J Biol Chem 1995;270:31016-31026.
36 Robinson NC, Huang P, Kaetzel MA, Lamb FS, Nelson DJ: Identification of an n-terminal amino acid of the clc-3 chloride channel critical in phosphorylation-dependent activation of a camkii-activated chloride current. J Physiol 2004;556:353-368.
37 Arreola J, Begenisich T, Nehrke K, Nguyen HV, Park K, Richardson L, Yang B, Schutte BC, Lamb FS, Melvin JE: Secretion and cell volume regulation by salivary acinar cells from mice lacking expression of the clcn3 cl- channel gene. J Physiol 2002;545:207-216.
38 Suzuki M, Mizuno A: A novel human Cl^- channel family related to drosophila flightless locus. J Biol Chem 2004;279:22461-22468.
39 Hussy N: Calcium-activated chloride channels in cultured embryonic xenopus spinal neurons. J Neurophysiol 1992;68:2042-2050.
40 Fahmi M, Garcia L, Taupignon A, Dufy B, Sartor P: Recording of a large-conductance chloride channel in normal rat lactotrophs. Am J Physiol 1995;269:E969-976.
41 Tsunenari T, Sun H, Williams J, Cahill H, Smallwood P, Yau KW, Nathans J: Structure-function analysis of the bestrophin family of anion channels. J Biol Chem 2003;278:41114-41125.
42 Marmorstein AD, Kinnick TR: Focus on molecules: Bestrophin (best-1). Exp Eye Res 2007;85:423-424.
43 Marmorstein LY, Wu J, McLaughlin P, Yocom J, Karl MO, Neussert R, Wimmers S, Stanton JB, Gregg RG, Strauss O, Peachey NS, Marmorstein AD: The light peak of the electroretinogram is dependent on voltage-gated calcium channels and antagonized by bestrophin (best-1). J Gen Physiol 2006;127:577-589.
44 Barro-Soria R, Schreiber R, Kunzelmann K: Bestrophin 1 and 2 are components of the Ca^{2+} activated Cl^- conductance in mouse airways. Biochim Biophys Acta 2008;1783:1993-2000.
45 Rosenthal R, Bakall B, Kinnick T, Peachey N, Wimmers S, Wadelius C, Marmorstein A, Strauss O: Expression of bestrophin-1, the product of the vmd2 gene, modulates voltage-dependent Ca^{2+} channels in retinal pigment epithelial cells. Faseb J 2006;20:178-180.
46 Yu K, Xiao Q, Cui G, Lee A, Hartzell HC: The best disease-linked cl- channel hbest1 regulates ca v 1 (l-type) Ca^{2+} channels via src-homology-binding domains. J Neurosci 2008;28:5660-5670.
47 Caputo A, Caci E, Ferrera L, Pedemonte N, Barsanti C, Sondo E, Pfeffer U, Ravazzolo R, Zegarra-Moran O, Galietta LJ: Tmem16a, a membrane protein associated with calcium-dependent chloride channel activity. Science 2008;322:590-594.
48 Yang YD, Cho H, Koo JY, Tak MH, Cho Y, Shim WS, Park SP, Lee J, Lee B, Kim BM, Raouf R, Shin YK, Oh U: Tmem16a confers receptor-activated calcium-dependent chloride conductance. Nature 2008;455:1210-1215.
49 Schroeder BC, Cheng T, Jan YN, Jan LY: Expression cloning of tmem16a as a calcium-activated chloride channel subunit. Cell 2008;134:1019-1029.
50 Schreiber R, Uliyakina I, Kongsuphol P, Warth R, Mirza M, Martins JR, Kunzelmann K: Expression and function of epithelial anoctamins. J Biol Chem;285:7838-7845.
51 Pifferi S, Dibattista M, Menini A: Tmem16b induces chloride currents activated by calcium in mammalian cells. Pflugers Arch 2009;458:1023-1038.

52 Sagheddu C, Boccaccio A, Dibattista M, Montani G, Tirindelli R, Menini A: Calcium concentration jumps reveal dynamic ion selectivity of calcium-activated chloride currents in mouse olfactory sensory neurons and tmem16b-transfected hek 293t cells. J Physiol;588:4189-4204.
53 Stephan AB, Shum EY, Hirsh S, Cygnar KD, Reisert J, Zhao H: Ano2 is the cilial calcium-activated chloride channel that may mediate olfactory amplification. Proc Natl Acad Sci USA 2009;106:11776-11781.
54 Stohr H, Heisig JB, Benz PM, Schoberl S, Milenkovic VM, Strauss O, Aartsen WM, Wijnholds J, Weber BH, Schulz HL: Tmem16b, a novel protein with calcium-dependent chloride channel activity, associates with a presynaptic protein complex in photoreceptor terminals. J Neurosci 2009;29:6809-6818.
55 Martins JR, Faria D, Kongsuphol P, Reisch B, Schreiber R, Kunzelmann K: Anoctamin 6 is an essential component of the outwardly rectifying chloride channel. Proc Natl Acad Sci USA 2011;108:18168-18172.
56 Schreiber R, Uliyakina I, Kongsuphol P, Warth R, Mirza M, Martins JR, Kunzelmann K: Expression and function of epithelial anoctamins. J Biol Chem 2010;285:7838-7845.
57 Duran C, Qu Z, Osunkoya AO, Cui Y, Hartzell HC: Anos 3-7 in the anoctamin/tmem16 cl- channel family are intracellular proteins. Am J Physiol Cell Physiol 2012;302:C482-493.
58 Hamill OP, Marty A, Neher E, Sakmann B, Sigworth FJ: Improved patch-clamp techniques for high-resolution current recording from cells and cell-free membrane patches. Pflugers Arch 1981;391:85-100.
59 Barry PH, Lynch JW: Liquid junction potentials and small cell effects in patch-clamp analysis. J Membr Biol 1991;121:101-117.
60 Pfaffl MW: A new mathematical model for relative quantification in real-time rt-pcr. Nucleic Acids Res 2001;29:e45.
61 Tian Y, Kongsuphol P, Hug M, Ousingsawat J, Witzgall R, Schreiber R, Kunzelmann K: Calmodulin-dependent activation of the epithelial calcium-dependent chloride channel tmem16a. Faseb J 2011;25:1058-1068.
62 Luther SA, Bidgol A, Hargreaves DC, Schmidt A, Xu Y, Paniyadi J, Matloubian M, Cyster JG: Differing activities of homeostatic chemokines ccl19, ccl21, and cxcl12 in lymphocyte and dendritic cell recruitment and lymphoid neogenesis. J Immunol 2002;169:424-433.
63 Ivanenko A, Baring MD, Airey JA, Sutko JL, Kenyon JL: A caffeine- and ryanodine-sensitive Ca^{2+} store in avian sensory neurons. J Neurophysiol 1993;70:710-722.
64 Hiraoka M, Kawano S, Hirano Y, Furukawa T: Role of cardiac chloride currents in changes in action potential characteristics and arrhythmias. Cardiovasc Res 1998;40:23-33.
65 Kuruma A, Hartzell HC: Dynamics of calcium regulation of chloride currents in xenopus oocytes. Am J Physiol 1999;276:C161-175.
66 Krause KH, Welsh MJ: Voltage-dependent and Ca^{2+}-activated ion channels in human neutrophils. J Clin Invest 1990;85:491-498.
67 Holevinsky KO, Jow F, Nelson DJ: Elevation in intracellular calcium activates both chloride and proton currents in human macrophages. J Membr Biol 1994;140:13-30.
68 Nishimoto I, Wagner JA, Schulman H, Gardner P: Regulation of Cl^- channels by multifunctional cam kinase. Neuron 1991;6:547-555.
69 Duffy SM, Lawley WJ, Conley EC, Bradding P: Resting and activation-dependent ion channels in human mast cells. J Immunol 2001;167:4261-4270.
70 Akita T, Fedorovich SV, Okada Y: Ca^{2+} nanodomain-mediated component of swelling-induced volume-sensitive outwardly rectifying anion current triggered by autocrine action of atp in mouse astrocytes. Cell Physiol Biochem 2011;28:1181-1190.
71 Liu HT, Akita T, Shimizu T, Sabirov RZ, Okada Y: Bradykinin-induced astrocyte-neuron signalling: Glutamate release is mediated by ros-activated volume-sensitive outwardly rectifying anion channels. J Physiol 2009;587:2197-2209.
72 Parekh AB, Putney JW Jr: Store-operated calcium channels. Physiol Rev 2005;85:757-810.
73 Manoury B, Tamuleviciute A, Tammaro P: Tmem16a/anoctamin 1 protein mediates calcium-activated chloride currents in pulmonary arterial smooth muscle cells. J Physiol 2010;588:2305-2314.
74 Hwang SJ, Blair PJ, Britton FC, O'Driscoll KE, Hennig G, Bayguinov YR, Rock JR, Harfe BD, Sanders KM, Ward SM: Expression of anoctamin 1/tmem16a by interstitial cells of cajal is fundamental for slow wave activity in gastrointestinal muscles. J Physiol 2009;587:4887-4904.